

### **Optic Lenses Manufactured on Fiber Ends**

#### Wenxin Zheng, Director of Engineering, Fusion Splicing, AFL

#### **ABSTRACT**

Different types of fiber lenses have formed a large family of fiber components in fiber laser, medical, and telecom industries. By using  $CO_2$  laser fusion technology, many components with extreme geometries and critical requirements, which were very hard to make in the past, can now be easily manufactured. These newly developed fiber lenses are reviewed and discussed for their merits and key features in this article.

**Keywords:** Fiber lens, components, laser beam, fusion

#### I. INTRODUCTION

Fiber optic based components are playing more and more critical roles in different fields such as fiber lasers used in medical operations and metal cutting industries, fiber sensors in environmental monitoring and alarming systems, and fiber signal transmission systems in telecom and surveillance. Among the many different fiber components, fiber lenses are receiving the most attention in all the three aforementioned fields. Fiber lenses are required for a variety of applications such as medical surgical, optical coherence tomography, viscosity detection probes, touchless optical switches, visible laser scanning imaging system, etc. In each of these applications, the fiber lenses can be shaped in various ways; i.e.: ball, elliptical, bending, and axicon shapes.

Since the lenses can be exposed to extreme powers (nW to kW), in different sizes (5  $\mu$ m to 2 mm diameter), and in large quantities, the repeatability and consistency are of high concern. Most traditional heating methods, (such as arc discharge, filament, and oxyhydrogen torch), are not suitable for those applications. A CO<sub>2</sub> laser is the optimal heating source for fiber lens manufacturing due to its cleanness, lower maintenance, and long term consistency.

In this article, the technologies for fiber lenses of many different types are introduced and discussed for their design, fabrication, and application.

#### **II. FIBER LENS AND BEAM GEOMETRY**

The major functionality of the lenses made at fiber ends is for realizing certain beam properties from the fiber end, including numerical aperture (NA), focus length (L), spot size ( $2w_{02}$ ), beam diverging angle ( $\theta_2$ ), and propagation direction ( $\phi$ ). Different from the traditional algorithm deducted from free space ray tracing theory to a standalone ball lens, the actual optical performance for a lens shaped on a fiber end is much more complicated. The NA, L, w, and  $\theta$  are all dependent on fiber types (such as SMF, MMF, LMA, etc.), lens shape (ball, truncated ball, elongated ball, tapered ball, axicon, etc.), lens material (fiber, pure fused silica, etc.), and splicing distance between the fiber and the lens surface (S). For example, using SMF28 fiber at 1550 nm wavelength, and varying the ball diameter and the splicing distance, one can achieve focus length L from a few microns to a few centimeters and a spot size from submicron to a few hundred microns. With multimode fibers (MMF) for medical applications, by varying lens tip curvature from a few microns to 2 mm, one can achieve a focus length from a positive value, to infinity (collimator), or to a negative value (beam diffusor) with the beam diverging angle ( $\theta_2$ ) from near zero to 180 degrees.

# FAFL

### **Fusion Splicing Systems**

In Fig. 1, a general geometry of fiber lens is described. The fiber lens can either be made using the beam transmission fiber or spliced with a different lens fiber. For achieving an accurate beam quality, pure silica fiber is often used to avoid beam perturbation by the dopant material in a transmission fiber. Depending on applications, the taper angle can either be positive (up-taper), negative (downtaper), or zero (straight). The tapered section can also be inside the beam transmission fiber with the splice point at the end of the taper. The tapered transmission fiber provides a possibility to achieve a desired output NA at the end of lens. The ball shape can also be a spherical ball,

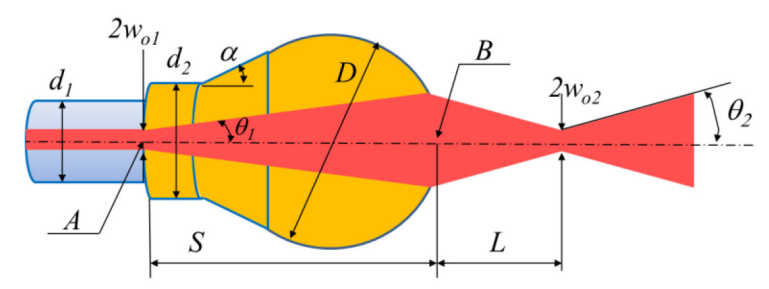


**Fig. 1:** Geometry of fiber lens and beam shape. D: ball diameter;  $d_1$ : transmission fiber diameter;  $d_2$ : lens fiber diameter;  $\alpha$ : taper angle; S: splice distance; L: beam focus length;  $2w_0$ : beam waist diameter of beam 1 inside the lens and beam 2 in the air;  $\theta$ . beam diverging angle of beam 1 and 2. Interface A denotes for the splice point between the fiber and lens, while interface B is between lens and air.

an elliptical ball, or a tapered cylinder with a flat tip, so the ratio of S/D can be ranged from a fraction to a few thousands. For a flat tip, D may go to infinity with S = 0, while for a sharp tip, D may only be a few microns.

#### **III. GAUSSIAN BEAM SIMULATION**

With the general geometry in Fig. 1, the beam propagation can be approximated with Fresnel approximation of the spherical wave where  $(x^2 + y^2)^2 << 4z^3\lambda$ . By assuming axial symmetry in cylindrical coordinates, the beam should meet the paraxial wave equation [1]

$$\frac{\partial^2 u}{\partial r^2} + \frac{1}{r} \frac{\partial u}{\partial r} - 2jk \frac{\partial u}{\partial z} = 0$$
 (1)

The simplest solution of the equation can be written in the form like a Gaussian distribution

$$u(r,z) = C(z)exp\left[\frac{-jkr^2}{2q(z)}\right] = 0$$
 (2)

where C and q are complex functions of z to be determined. By substituting u in Eq. (2) into the paraxial wave equation (1), separating the dependent on r and z, and solving the individual equations, we obtain the expression of the complex beam parameter q(z) as [1]

$$\frac{1}{a} = \frac{1}{R} - \frac{j\lambda}{\pi w^2} \tag{3}$$

$$R = z + \frac{z_r^2}{z} \tag{4}$$

$$w = w_0 \sqrt{1 + \left(\frac{z}{z_r}\right)^2} \tag{5}$$

$$\tan \theta_0 = \frac{w_0}{z_r} = \frac{\lambda}{n\pi w_0} \tag{6}$$

$$z_r = \frac{n\pi w_0^2}{\lambda} \tag{7}$$

Where R(z) represents for radius of curvature of a spherical wave front, w(z) for beam radius at which the field falls to  $1/e^2$  relative to its peak value,  $w_0$  for radius of the beam waist,  $\theta_0$  for asymptotic beam growth angle in the far field  $z >> z_r$ ,  $z_r$  for the Rayleigh range, and n for refractive index where the beam is propagating.



For the fiber lens structure shown in Fig. 1, the incident beam from the fiber loses its guidance at the interface A. Assuming the lens consists of a uniform material which has the same refractive index n of fiber glass, the beam will propagate inside the lens with its beam waist  $2w_{0l}$  at the fiber end A and asymptotic angle  $\theta_l$ . At the interface B at the lens surface, the beam is refracted to form a new beam propagating in the air. In general, the new beam waist  $2w_{0l}$  and asymptotic angle  $\theta_l$  need to be computed numerically point by point based on Snell's Law along the interface B. For only a few simple cases, the relation between beam 1 and beam 2 can be expressed analytically. A few examples are discussed in the following sub-sections.

#### A. Spherical Lens With Single-Mode Fiber

For the cases that the fiber is single-mode fiber (SMF), the lens curvature is constant at interface B with radius  $\rho = D/2$ , the lens neck  $d_2$  is wide and short which does not confine the beam 1 for Numerical Aperture (NA) conversion, the taper angle is larger or equal to 0, then the beam 1 inside the lens can be described by a Gaussian beam with its waist at fiber end A, its spot size  $2w_{01}$  equal to mode field diameter (MFD) of the SMF, and its radius of curvature of a spherical wave front  $R_1$  given by Eq. (4).

$$R_1 = S + \frac{\left(\frac{n\pi w_{01}^2}{\lambda}\right)^2}{S}$$

With the knowledge of  $w_{01}$  and  $R_{11}$ , the focus length L and spot size of the beam 2,  $2w_{02}$ , can be expressed in an analytically form [2]:

$$L = \frac{-R_r \omega_r^2}{\pi \omega_r^2 + \lambda - R_r} \tag{8}$$

$$w_{02} = \frac{\omega_r}{\sqrt{1 + \left(\frac{\pi \omega_r}{\lambda R_r}\right)^2}} \tag{9}$$

Where

$$R_r = \frac{1}{\text{Re}\left(\frac{1}{a}\right)} \tag{10}$$

$$\omega_r = \sqrt{\frac{-\lambda}{\pi \operatorname{Im}\left(\frac{1}{q_r}\right)}} \tag{11}$$

$$q_r = \frac{q\rho}{(1-n)q+n\rho} \tag{12}$$

$$q = 1 / \left( \frac{1}{R_1} - \frac{j\lambda}{n\pi w_{01}^2} \right) \tag{13}$$

Although having the analytical expression, the actual relationship between the lens design parameters S,  $\rho$ , and the optical performance  $2w_{\theta 2}$ , L, and  $\theta_2$  still need to be calculated numerically.

#### **B.** Cylindrical Hyperbolic Lenses

For a real optical component, the actual lens surfaces at B are not perfect spherical, i.e., the surface curvature radius  $\rho$  is not a constant. This is especially true when the fiber lens is designed with a sharp down taper ( $\alpha << 0$ ) for laser diode coupling, the lens surface is of



cylindrical hyperbolic shaped. In this case, the curvature radius  $\rho$  varies point by point with rotational symmetric. However, the hyperbolic profile can be defined by its minimum radius  $\rho_m$  and the wedge angle  $\beta$  between the asymptotes. Assuming  $\beta$  is fixed at its aberration-free wedge angle, the beam 2 can be explicitly expressed by the beam 1 characteristics [3]:

$$w_{02} = \left(\frac{w_{01}\rho_m}{n-1}\right) / \sqrt{\left(\frac{\rho_m}{n-1}\right)^2 + \left(\frac{\pi w_{01}^2}{\lambda}\right)^2}$$
 (14)

$$L = \left(\pi w_{02} \sqrt{w_{01}^2 - w_{02}^2}\right) / \lambda \tag{15}$$

For a small radius of lens curvature, where

$$\rho_m \ll \frac{\pi w_{01}}{\lambda} (n-1) \tag{16}$$

the waist diameter in the air,  $2w_{02}$ , is proportional to the lens radius of curvature and inversely proportional to the fiber MFD

$$w_{02} = \frac{(n-1)\lambda \rho_m}{\pi w_{01}} \tag{17}$$

and

$$L = \frac{\rho_m}{n-1} \tag{18}$$

For example,  $w_{oI} = 5 \mu m$  for SMF28 at 1.55  $\mu m$  wavelength with n = 1.46, to meet Eq. (16) the lens radius  $\rho_m$  should be much smaller than 4.6  $\mu m$ . So, the approximation Eq. (17) and (18) should be used carefully on the condition Eq. (16).

#### C. Fiber Lens With Multimode Beam Incidence

In the case that the fiber can carry beams of multimode or a few modes, the analytic expression for the beam propagation is very difficult to be obtained. Although each mode may still meet the equations discussed in the above subsections A and B, the beam integration may need great effort for analyzing.

However, for multimode propagation of the fiber core radius and lens dimensions have to be much larger than the wavelength. That leads to more application of ray tracing method and NA analyzing method than for the cases of single mode situation. The beam 1 can be thus approximated by a group ray from zero NA to the maximum NA the fiber can carry. The rays meet Snell's Law at each point of the lens surface B. The integration of the rays in the air forms the beam 2. Although it's hard to give analytic solutions, with the ray tracing method, it is still possible to get reasonably good simulation on L and  $\theta_2$ .

#### IV. FIBER LENS APPLICATIONS

Fiber lenses of different types have wide applications in many areas as discussed in section I. A few examples are studied and illustrated with actual products in this section.

#### A. Touchless Connection

Touchless connectors are key components in high speed optical switches, MEMS system for optical networks, and high power fiber



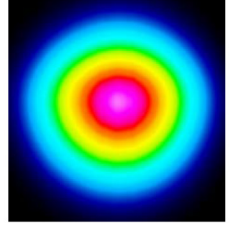


**Fig. 2.** 80 µm SMF with a ball lens (D=679 µm,  $d_1=80$  µm,  $d_2=251$  µm) with measured L=7.5 mm,  $2w_{02}=137$  µm, coupling loss =0.8 dB, and return loss =34 dB without an anti-reflection coating. The beam shape was measured at the waist with  $\lambda=1550$  nm.



laser systems. By varying ball diameter D, ratio of S/D, and taper angle  $\alpha$ , output beam waist  $2w_{02}$  and focus length L can be adjusted to almost any desired value for a SMF input. The power density at the glass-air interface B can also be reduced significantly by using a large S and D to avoid glass burning by too high power intensity.

#### **B. Ball Shaped End-cap for Fiber Laser Systems**

End-caps of different types are widely used in fiber laser systems to reduce the fiber facet damage threshold and the back reflection. Most of commercial end-caps consist of a cylindrical rod of fused silica with flat or angle polished end-surface. By fusion splicing the end cap to the output fiber, the laser beam defuses, and the spot size enlarges inside the end-cap. Thus, the power density at the air-silica interface is much lower compared to the case without end-capping. However, with the traditional cylindrical rod shape, the beam divergent angle is not quite controllable due to its flat (or angled) end surface. For many applications (such as medical surgery, metal cutting, etc.), less diverged, collimated, or focused beams are required and ball shaped end-caps should be developed.

A large number of ball lenses are made on MMF and SMF for NA measurement, where there are no necks between the fiber and ball, i.e.  $S\!/\!D = 1$ . The MFD of the SMF is about 10  $\mu$ m and the NA of the 125  $\mu$ m core diameter MMF is about 0.47. All data were obtained with far field measurement using Eq. (6) at 1550 nm wavelength. The test results are shown in Fig. 3. We can observe that the ball lens at a fiber end functions as an NA converter. To achieve a smaller NA (larger spot size and longer focus length), a larger ball size is needed. However, by slightly increasing the ratio of  $S\!/\!D$ , one can also achieve a larger spot size without significantly increasing the ball size (as described by Eq. (9)). More discussions and examples will be published in a separated paper on this topic [4].

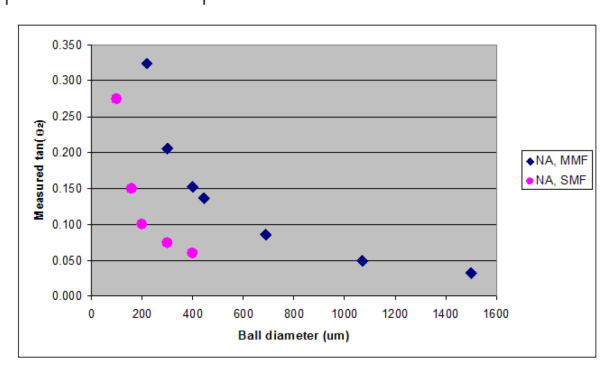
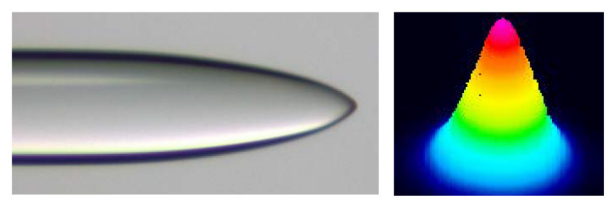


Fig. 3. Measured numerical aperture, NA  $\approx tan(\theta_2)$  for MMF and SMF with  $S\!\!\!/D=1.$ 

#### C. Fiber and Laser Diode Coupling

From Fig. 3 in subsection B, we can observe that for achieving a very small spot size (large NA) the lens radius has to be very small. To manufacture such a fiber lens with a small radius, a piece of down taper ( $\alpha$  < 0) is necessary. This type of ball lens is also referred to as an axicon shaped fiber lens, or hyperbolic lenses. The small spot size (and large acceptance NA) is an ideal coupler from the laser diode to fiber. One typical axicon example is shown in Fig. 4. Measured NAs and waist spot sizes of different down-tapered axicons lenses are shown in Fig. 5.



**Fig. 4.** 125  $\mu$ m SMF28 with axicon tip ( $D \approx 8 \mu$ m,  $d_I = 125 \mu$ m,  $L = 13 \mu$ m,  $w = 2.4 \mu$ m) and beam shape measured at 1 mm from tip at 1550 nm wavelength.

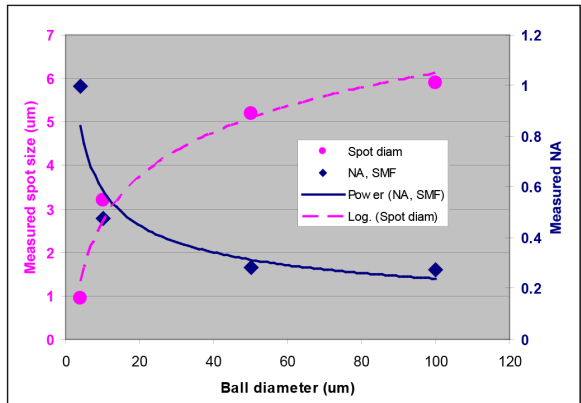


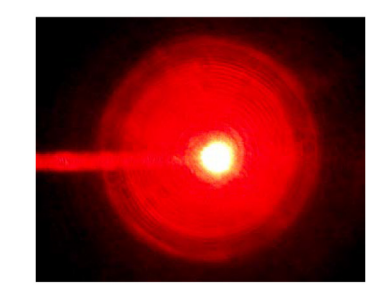
**Fig. 5.** Measured numerical aperture and waist spot size from far field measurement method Eq. (6) for a few axicons with different minimum radius  $\rho_m$  of the hyperbolic lenses. The asymptotic ball diameter  $D=2\rho_m$  at lens tip.



#### D. Tissue Ablation Diffusor

The beam diffusing tip is a key component to ablate tissue in the human body. This process has, to a large extent, cured epilepsy in young people, and has made small tumor brain surgery a two-hour outpatient surgery. To diffuse the beam in all directions, the output beam NA has to be extremely large. The data shown in Fig. 5 implies that an axicon lens with extremely small tip radius will work as a diffusor with SMF.

For MMF, a sharp down taper will also work for a diffusor. When  $\alpha < 0$ , the total reflection condition between cladding  $(n_1)$  and core  $(n_2)$  become  $\sin(\pi/2 - \theta - \alpha) = n_1 / n_2$ , where  $\theta \approx \text{NA}$  and



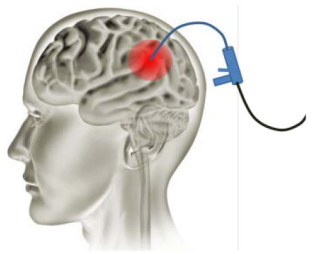


**Fig. 6.** 125 µm SMF28 with tapered lens ( $D \approx 4$  µm,  $d_1 = d_2 = 125$  µm,  $\theta_2 = 180$  deg) with similar lens shape as shown in Fig. 4. The operation is normally with 980 or 1060 nm wavelength. The left picture was taken with red laser.

 $\theta^2 \approx n_2^2 - n_1^2$  for MMF. So, to keep the fiber from leaky, the absolute  $\alpha$  value has to meet:

$$|\alpha| \le \frac{\pi}{2} - \sin^{-1}\left(\frac{n_1}{n_2}\right) - \sqrt{n_2^2 - n_1^2}$$
 (19)

However, to make a diffusor, we may intentionally select a large  $\alpha$  value to make the fiber tip very leaky.

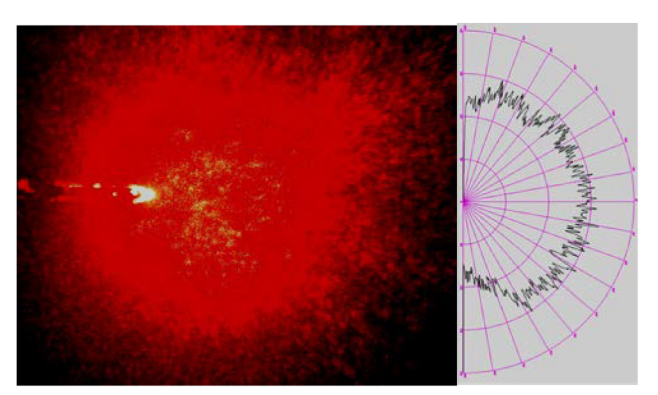


**Fig. 7.** 400 µm core MMF with tapered lens ( $D \approx 4$  µm,  $d_1 = d_2 = 400$  µm,  $\theta = 180$  deg) with similar lens shape as shown in Fig. 4. The operation is normally with 980 or 1060 nm wavelength. The left picture was taken with red laser. The right picture is measured light intensity at different angle with Photon profiler.

**Fig. 8.** 300 µm MMF with ball lens (D=1008 µm,  $d_1=300$  µm,  $d_2=400$  µm, L=350 µm,  $2w_{o2}=201$  µm) operation at 1060 nm wavelength. Top: a typical laser surgery knife with ball lens blade. Left: ball lens tip magnified. Right: Ball lens image shown is made by fusion splicer.

### E. Laser Surgery Blade

A typical laser blade for eye surgery is often made with a very large ball. The short focus length is achieved in air. When the ball tip touches the eye fluid, the focus length becomes a few millimeters long and suitable for the operation due to the refractive index,  $n_I$ , is about 1.3 for water and 1 for air.

#### F. Side Fire Kidney Stone Removing

Bent tip ball lens is one method for side fire in laser treatment of kidney stone removal. The surgery uses ureteroscope, which provides a video image and has small "working" channels, inserted into the bladder and up the ureter until the stone is





**Fig. 9.** 125 µm SMF28 with bent lens (D=150 µm,  $d_1=d_2=125$  µm, L=400 µm,  $2w_{o2}=20$  µm,  $\phi=30$  deg). The ball lens picture was taken and stitched automatically by Fiber Processing Software for PC. The entire lens fabrication process is about 1 minute and fully automated.

encountered. The stone can then be broken up with a high power fiber laser using either straight or bent tips fiber lenses.



#### V. FIBER LENS MANUFACTURING

There are many different methods and equipment available commercially for making fiber lenses. For a simple ball lens of 300  $\mu$ m or less, people can make them with fusion splicers designed for factory operations, but for more complicated fiber lenses, or when large diameter fibers are involved, a more advanced fiber processing station has to be considered. Four major types of heat sources have been developed for advanced fiber processors. They are flame type with hydrogen oxygen burner, arc discharge type with two or multiple electrodes, filament type with omega shaped tungsten or graphite filament and inner gas for protection, and  $CO_2$  laser type. The pros and cons of all the four types of heating sources are listed in Table 1 for comparison.

	Flame			CO <sub>2</sub> Laser
METHOD	Flame Torch	Electrode Arc Discharge	Filament Heater	CO <sub>2</sub> Laser
YEAR INTRODUCED FOR FIBER HEATING	Late 1960s	2 electrodes—1970s     Multiple electrodes—     mid 1980s by NTT	1990	Late 1980s
PRO	Wide heating range (~5 mm)	No need for gas supply	No need for high voltages	Cleanest with no deposits on fiber
CON	<ul><li>Need gas supply system for flame</li><li>High water peak absorption</li></ul>	<ul> <li>Need to clean electrodes after every taper if fiber OD &gt;1.5 mm</li> <li>Deposit on fibers when electrodes are not clean</li> </ul>	<ul> <li>Need change filament after         ~50 min of use</li> <li>Filament deposits on fiber</li> <li>Filament alignment issues</li> </ul>	Need eye safety and other considerations

**Table 1**—Comparison of heating methods for fiber lens fabrication

Since the fiber lenses are used mainly with high power fiber lasers, the higher power levels present significant challenges in terms of power management and the avoidance of power leakage with resultant localized heating. Robustness and reliability of high power assemblies is therefore a greater concern. The use of a CO<sub>2</sub> laser as a heat source has only recently become commercially available for optical fiber splicing and component fabrication. CO<sub>2</sub> laser heating is different from other heating methods in that the power from the CO<sub>2</sub> laser beam is absorbed by the outer layer of the glass, which in turn conducts the energy inward. In this case, there is no consumable heating element, such as electrodes or resistive filaments, that may leave contaminants or deposits on the glass surface. The CO<sub>2</sub> absorptive heating can also be a very well controlled process, with minimal vaporization and re-deposition of the glass itself. Heating by a CO<sub>2</sub> laser results in a contamination-free glass surface, with little surface damage or irregularity. Since the glass surface is very smooth and contamination-free, high power may be utilized in the component without localized surface hot spots, power leakage, loss of efficiency, and significant heat management problems.

After carefully comparing the listed heating methods, the  $CO_2$  laser glass processing station LZM-100 (see Fig. 10) is chosen for our fiber lens fabrication due to the following considerations:

- Large diameter fiber splicing and ball-lensing needs long heating times at high power levels. Both of these attributes can cause degradation
  of electrodes and filaments while also increasing the risks of cladding surface contamination and power leakage. Said risks don't exist with
  a CO<sub>2</sub> laser splicer.
- Many types of fiber lens products are one time use only, especially for medical surgery. Higher quantity and lower cost of each component
  is thus a great concern. With arc discharge machines, electrodes need to be cleaned or replaced very often when the ball lens diameter
  is larger than 300 μm. When larger than 700 μm, the electrodes have to be cleaned for every operation, but with CO<sub>2</sub> laser heating, the
  maintenance and related downtime is reduced significantly.
- The initial cost for a CO<sub>2</sub> laser machine is typically higher than an electrode or a filament machine, but there are essentially no recurring consumable costs and no downtime cost for a laser machine calibration due to changing of electrodes or filaments. The total cost of



ownership (initial cost + consumable costs) is typically much higher for both the electrode and filament machines than that of the  $CO_2$  laser machine.

 Product consistency is another major concern for fiber lens manufacturing. It is not only related to the production yield and cost, it is also a main contributor of product quality. The recently developed real time feedback control system [5] makes it much more stable than most of CO<sub>2</sub> laser can originally provide. LZM-100 has actually integrated most of the splicing and fiber processing technologies developed in the last 20 years [6-11], and it provides a flexible and stable platform for fiber lens fabrication.

With the  $CO_2$  laser glass processing station LZM-100, many processes have been established for lens fiber production. All of them are automated with preset parameters. A few typical processes are discussed below.

#### A. Process of Ball Lens Fabrication with Single Fiber

Within all processes, the ball lens using single fiber is the easiest one and it was developed many years ago. By feeding the stripped fiber into a heat zone, which is created either by electrodes or CO<sub>2</sub> laser with high power, the glass melts and a ball is formed by surface tension illustrated by Fig. 11. To overcome the gravity impact for horizontally placed fiber, constant fiber rotation is necessary especially if the ball diameter is larger than 2X the fiber diameter. For vertically placed fibers, it is very difficult to overcome the gravity impact. As such, the shape of the resulting ball lens is more of a rain drop or mushroom shape vs. spherical.



**Fig. 10.** Fujikura's LZM-100 glass processing station for fiber diameter ranged from 5 μm to 2.3 mm, tapering length up to 130 mm, and fiber melting temperature ranged from 100°C to more than 2,000°C.

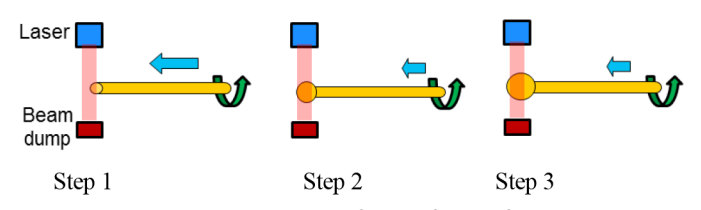


**Fig. 11.** Ball lens processing with single fiber by feeding fiber to heat zone with preset speed and constant rotation. The feeding length is calculated targeting to desired ball size. The ball size can be measure in real time during the process, and the laser power is a real time function of the ball size.

However, single fiber ball lens have limited applications due to its optical performance. (1) Using transmission fiber as the ball material leads to a random mixture of core and cladding material which induces perturbation to beam propagation, especially for MMF. (2) Ratio S/D = 1 becoming constant limits adjustability of spot size and output NA. (3) It may not work for large ball sizes where  $D/d_1 > 3$ .

## B. Process of Ball Lens Fabrication with Two Different Fibers

By splicing a lens-fiber (coreless fiber) to the transmission fiber before making a ball lens, one can solve the major issues which occur by using a single fiber only. In this case, the ball lens and/or taper are made with a pure silica fiber in a single process show in Fig. 12. After

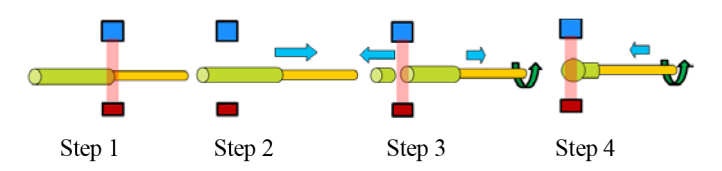


**Fig. 12.** Ball lens processing with both lens-fiber and transission fiber. The splicing, fiber breaking, and the ball lensing are processed in a sigle run. The ball size and desired S/D ratio are all pre-calculated and preset as program parameters.

splicing the fibers with different material and different sizes, the spliced fiber is moved toward the lens-fiber side to a pre-calculated distance. A strong laser power is applied to burn the lens fiber apart, then the ball lensing process starts on the lens fiber instead of the transmission fiber. The ball size and desired S/D ratio are all pre-calculated with very good repeatability.

In both process A and B, the relationship between feeding length I and ball diameter D is critical. The most intuitive relation should be from The Law of Conservation of Mass. However, the evaporated fiber material during the process should not be ignored. If we denote v as the evaporated volume of the glass, we have

$$\pi d_2^2 l = \frac{4}{3} \pi \left(\frac{D}{2}\right)^2 + v \tag{20}$$



Where  $d_2$  is the diameter of the lens-fiber (see Fig. 1). Improperly overheating during the ball lensing can result in a large value of v, especially for the case of  $CO_2$  laser heating. When the ball grows in the laser beam, it absorbs more and more energy during its increasing cross section. If the laser beam power is not reduced properly with the increasing ball diameter during the process, we will see v is not ignorable and ball size D will be much smaller than the expectation.

The fiber feeding speed should also be optimized. Too low speed increases the processing time and thus the costs in a production line. Conversely, too fast of a speed may heat the ball neck to cause the bending tip even with rotation. For parameter optimization before going to production lines, achieving a balanced solution may often need significant work.

#### C. Process for Axicon Lens Fabrication

Fabricating axicon fiber lens involves more complicated procedure and more accurate power control, due to the sensitivity of the axicon tip curvature radius  $\rho_m$  and the taper angle  $\alpha$  ( $\alpha$  < 0). The general fabrication process is illustrated in Fig. 13. As discussed a few times, CO<sub>2</sub> laser heating depends on abortion cross section. To fire polish the axicon tip, a higher power is required due to the small size of the tip (a few microns), but the higher power may damage the taper which has a larger diameter. Thus, a ball lens is created using the left side fiber. The heat radiation from the ball lens can polish the axicon tip effectively.

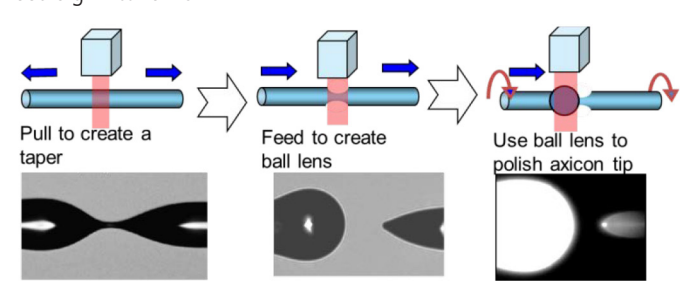


**Fig. 13.** Axicon lens processing illustration with both lens-fiber and transission fiber. The steps for splicing and moving are not shown due to the similarity to Steps 1 and 2 in Fig. 12. Fiber tapering, breaking, and the ball lensing for fire polishing are shown above. All steps are processed in a single run. The tip radius and desired *S/D* ratio are all pre-calculated and controlled by beam power and precision moving.

Similar to ball lensing, the axicon lens can also be made with single

transmission fiber only or made with a spliced pure silica lens-fiber. However, the optical performance from these two processes is very different for SMF. In the single fiber process, the core was tapered in the same ratio as cladding and the light eventually guided by the air at the tip as described by formulae in section III B. In contrary, with the two fiber processes, the light loses guidance at the splice point and propagates in the lens with diverge angle  $\theta_I$ . The entire section of the lens works as a tapered multimode fiber with the air acting as cladding. At the tip of the axicon, the output NA can be extremely large with NA =  $\theta_I$  +  $|k \times \alpha|$ , where k is the number of bouncing back and forth before the ray escape from the lens. Thus, instead of a diode couple, we achieve a diffusor shown in Fig. 6.

#### D. Process for Up-Taper Lens Fabrication

Process for axicons is an example of down-taper lens fabrication. Up-tapered lens are more often required for end-caps in fiber laser systems. Fig. 14 illustrates a general process of making such fiber lenses.

With the up-taper lensing techniques, one can actually create an elongated (oval) ball lens shown in Fig. 15.

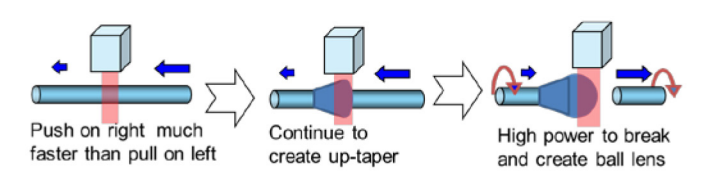


**Fig. 14.** Up-taper lens processing illustration with both lens-fiber and transission fiber. The steps for splicing and moving are not shown due to similarity to Steps 1 and 2 in Fig. 12. Fiber up-tapering, breaking, and the ball lensing are shown above. All steps are processed in a sigle run. The ball radius and desired S/D ratio are all pre-calculated and controlled by beam power and precision moving.

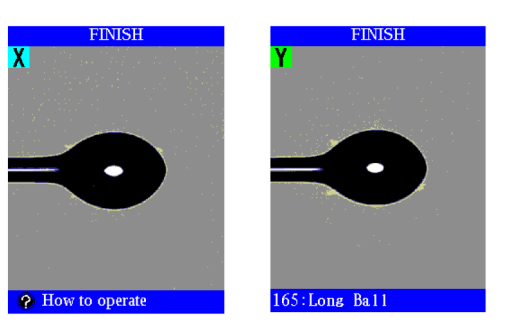


**Fig. 15.** Screen shots from LZM-100 for a elongated ball lens frabricated with up-taper lens process. The elongated ball lens has its long axis 500  $\mu$ m and short axis 300  $\mu$ m. The entire process is with a signle run. The X-view and Y-view images are taken by two cameras perpedicular to each other.



#### VI. SUMMARY

Fiber lensing technology is reviewed in different areas including theory, application, fabrication, and production equipment. Thanks to the boom in fiber laser system development, the applications of fiber lenses of different types are quickly penetrating in more and more fields, and the requirements on fiber lenses are also growing fast in quantity, quality, and variety of geometry designs.

With the very flexible and repeatable  $CO_2$  laser fiber processing platform, many new processes and products are successfully developed and many are still under development.

#### **ACKNOWLEDGMENT**

The author is particularly grateful for the guidance and continue support of Steve Althoff, VP of AFL's Equipment business. The author also thanks Doug Duke, Brad Hendrix, and Amine Jebali for instructive discussions in the entire development work.

#### **REFERENCES**

- [1] Bahaa E. A. Saleh, Malvin Carl Teich, "Fundamentals of Photonics," Copyright 1991 John Wiley & Sons, Inc., Published Online: 4 DEC 2001.
- [2] G. Wu, A. R. Mirza, S. K. Gamage, L. Ukrainczyk, N. Shashidhar, G. Wruck3 and M. Ruda, "Design and use of compact lensed fibers for low cost packaging of optical MEMS components", J. Micromech. Microeng. 14 (2004), pp. 1367-1375.
- [3] N. Axelrod, A. Lewis, N. B. Yosef, R. Dekhter, G. Fish, and A. Krol, "Small-focus integral fiber lenses: modeling with the segmented beam-propagation method and near-field characterization," in APPLIED OPTICS, vol. 44, No. 7, March, 2005, pp. 1270-1282.
- [4] W. Zheng, "Ball Shaped End-caps for Fiber Laser Systems," unpublished.
- [5] W. Zheng, H. Sugawara, T. Mizushima, and W. Klimowych, "Heating power feedback control for CO<sub>2</sub> laser fusion splicers," Photonics West Technical Digest, #8601-79, 2013.
- [6] Y. Noguchi, K. Nishiwaki, K. Oda, H. Tanaka, K. Asano, T. Matsuura, H. Hosoya, "Subminiature micro-optic devices with mini quartz-rod-lens", Fujikura Technical Review, pp 5-9, 2004.
- [7] W. Zheng, B. Malinsky, "Arc Power Calibration for Fusion Splicing," Proc. of SPIE Vol. 8237 paper 82372E, San Francisco, (2011).
- [8] D. Duke, W. Zheng, H. Sugawara, T. Mizushima, and K. Yoshida, "Plasma zone control for adaptable fusion splicing capability," Proc. SPIE, Photonic West (2012).
- [9] W. Zheng, "Real time control of arc fusion for optical fiber splicing," IEEE J. Lightwave Tech., Vol.11, No. 4, pp. 548-553, 1993.
- [10] K. Inoue, K. Sasaki, Y. Suzuki, N. Kawanishi, and Y. Tsutsumi, "Method for fusion splicing optical fiber and fusion splicer," US Patent 6,294,760, Fujikura, Sept. (2001).
- [11] M. Harju, H. Sugawara, T. Mizushima, "Electron spectroscopy studies on magneto-optical media and plastic substrate interface," Photonics West Technical Digest, Proc. of SPIE Vol. 8961, 89613C-7, 2014.